DOI 10.1007/s10891-015-1162-1

Journal of Engineering Physics and Thermophysics, Vol. 88, No. 1, January, 2015

DYNAMICS OF A COAGULATING POLYDISPERSE GAS SUSPENSION IN THE NONLINEAR WAVE FIELD OF AN ACOUSTIC RESONATOR

A. L. Tukmakov

UDC 539.37

A model of a multivelocity multitemperature polydisperse gas suspension has been constructed with account taken of coagulation. Calculations of the dynamics of an aerosol of a polydisperse composition in an acoustic resonator have been done and the derived regularities have been described. A system of Navier–Stokes equations for a compressible heat-conducting gas was used to describe the motion of a carrier medium. The dynamics of dispersed fractions is described by a system of equations including continuity, momentum, and internal-energy equations. The equations of motion of the carrier medium and dispersed fractions have been written with account of the interphase exchange of momentum and energy. The Lagrangian model has been used to describe the process of coagulation. The change in the dispersity of the gas suspension in the nonlinear field of an acoustic resonator has been analyzed.

Keywords: *acoustic resonator, Navier–Stokes equations, equations of motion of a polydisperse gas suspension, McCormack explicit scheme, nonlinear and discontinuous vibrations, coagulation of particles.*

Introduction. There are technologies of gasification of cryogenic liquids and of purification and desalination of water that are based on adiabatic expansion of the liquid in nozzles [1]. One basic stage in these processes is the separation of the phases of a vapor-gas dropping liquid formed at the nozzle exit with the aid of inertial-type separators. A distinctive feature of such separators is that particles of the order of one micron or smaller in radius are not separated from the carrier medium; for the quality of phase separation to be improved, it is required that the particle distribution by size be changed by decreasing the concentration of fine fractions. One method of solution of this problem involves acoustic action, on the medium, by nonlinear wave fields increasing the rate of coagulation of droplets. Selection of the intensity of the wave action is limited by the critical Weber number [2].

Gas suspensions may have, as part of them, particles of different size r with a certain distribution function $N(r)$. To model the dynamics of such a mixture one uses different approaches. In some case a description of the dynamics of a polydisperse mixture can be based on the model of a monodisperse gas suspension consisting of particles with a certain effective radius a_* which is selected according to the generalized formula

$$a_* = a_{m,n} = \left[\frac{\int_{a_{\min}}^{a_{\max}} N(r) r^m dr}{\int_{a_{\min}}^{a_{\max}} N(r) r^n dr} \right]^{\frac{1}{(m-n)}}, \quad a_{m,n} = a_{n,m}, \quad m \neq n .$$

As has been shown in [3, 4], the radii $a_{5,3}$ and $a_{3,1}$ are used to describe the propagation of longwave and shortwave acoustic disturbances respectively, whereas the radius $a_{4,3}$ is selected as the equivalent radius for waves of intermediate length. Polydisperse models are required for a more exhaustive account of the actual size distribution of particles. A mathematical model of a polydisperse gas suspension, in which to each particle size there corresponds its own fraction, has been given in [4]. The carrier phase is described by a system of Navier–Stokes equations with account of the exchange of momentum and energy with all the dispersed fractions. Thus, the dispersed phase includes n fractions, each being described by a system of the continuity equation for the average density, equations of conservation of momentum components, and the internal-energy equation.

A. N. Tupolev Kazan National Research Technical University, 10 K. Marx Str., Kazan, Tatarstan, 420111, Russia; email: tukmakov@mail.knc.ru. Translated from Inzhenerno-Fizicheskii Zhurnal, Vol. 88, No. 1, pp. 11–19, January–February, 2015. Original article submitted June 19, 2014.

Each fraction exchanges momentum and energy with the carrier medium. To describe the process of coagulation of particles of different radii, use has been made of the Lagrangian model, which makes it possible to take account of the exchange of mass, momentum, and energy between fractions as a result of the collision of the particles [2].

Equations of Motion of a Multivelocity Multitemperature Polydisperse Gas Suspension. As the carrier medium, we consider a gas whose motion is described by a system of Navier–Stokes equations. A system of equations of motion of a multivelocity multitemperature gas suspension includes a system of equations of motion of the carrier phase and n systems of equations of motion of dispersed phases. In Cartesian coordinates, in a two-dimensional statement, the systems have the form [4, 5]

$$\frac{\partial \rho}{\partial t} + \frac{\partial (\rho u)}{\partial x} + \frac{\partial (\rho v)}{\partial y} = 0,$$

$$\frac{\partial (\rho u)}{\partial t} + \frac{\partial}{\partial x}\left(\rho u^2 + p - \tau_{xx}\right) + \frac{\partial}{\partial y}\left(\rho uv - \tau_{xy}\right) = -\sum_{i=1,n} F_{xi} + \alpha \frac{\partial p}{\partial x},$$

$$\frac{\partial (\rho v)}{\partial t} + \frac{\partial}{\partial x}\left(\rho uv - \tau_{xy}\right) + \frac{\partial}{\partial y}\left(\rho v^2 + p - \tau_{yy}\right) = -\sum_{i=1,n} F_{yi} + \alpha \frac{\partial p}{\partial y},$$

$$\frac{\partial (e)}{\partial t} + \frac{\partial}{\partial x}\left(\left[e + p - \tau_{xx}\right] u - \tau_{xy} v + \lambda \frac{\partial T}{\partial x}\right) + \frac{\partial}{\partial y}\left(\left[e + p - \tau_{yy}\right] v - \tau_{xy} u + \lambda \frac{\partial T}{\partial y}\right) \tag{1}$$

$$= -\sum_{i=1,n} Q_i - \sum_{i=1,n}\left(\left|F_{xi}\right|(u - u_i) - \left|F_{yi}\right|(v - v_i)\right) + \alpha\left(\frac{\partial pu}{\partial x} + \frac{\partial pv}{\partial y}\right),$$

$$p = (\gamma - 1)\left(e - \rho\left(u^2 + v^2\right)\Big/2\right), \quad e = I + \rho\left(u^2 + v^2\right)\Big/2, \quad \alpha = \sum_{i=1,n} \alpha_i$$

$$\tau_{xx} = \mu\left(2\frac{\partial u}{\partial x} - \frac{2}{3}D\right), \quad \tau_{yy} = \mu\left(2\frac{\partial u}{\partial y} - \frac{2}{3}D\right), \quad \tau_{xy} = \mu\left(\frac{\partial \mu}{\partial y} + \frac{\partial v}{\partial x}\right), \quad D = \frac{\partial u}{\partial x} + \frac{\partial v}{\partial y}.$$

Here ρ, u, v, u_i, v_i, e, λ, and μ are the density, the components of the velocity of the carrier and dispersed phase, the total energy, and the thermal conductivity and the coefficient of viscosity of the carrier phase. The quantities F_{xi}, F_{yi}, and Q_i are determined by the laws of interphase friction and heat transfer, and the internal gas energy is equal to $I = RT/(\gamma - 1)$.

The dynamics of each component of the dispersed phase is described by the equation of conservation of the average density of the dispersed phase and by the equations of conservation of the components of momentum and internal energy [4]:

$$\frac{\partial \rho_i}{\partial t} + \frac{\partial (\rho_i u_i)}{\partial x} + \frac{\partial (\rho_i v_i)}{\partial y} = 0,$$

$$\frac{\partial (\rho_i u_i)}{\partial t} + \frac{\partial}{\partial x}(\rho_i u_i^2) + \frac{\partial}{\partial y}(\rho_i u_i v_i) = F_{xi} - \alpha \frac{\partial p}{\partial x},$$

$$\frac{\partial (\rho_i v_i)}{\partial t} + \frac{\partial}{\partial x}(\rho_i u_i u_i) + \frac{\partial}{\partial y}(\rho v_i^2) = F_{yi} - \alpha \frac{\partial p}{\partial y}, \tag{2}$$

$$\frac{\partial (e_i)}{\partial t} + \frac{\partial}{\partial x}(e_i u_i) + \frac{\partial}{\partial y}(e_i v_i) = \mathrm{Nu}_i \frac{6\alpha_i}{(2r_i)^2}\lambda(T - T_i),$$

$$\rho_i = \alpha_i \rho_{i0}, \quad e_i = \rho_i C_{pi} T_i, \quad \alpha = \sum_{i=1,n} \alpha_i.$$

Here α_i, ρ_i, e_i, and T_i are the volume content, the average density, the internal energy, and the temperature of the dispersed phase, and C_{pi} and ρ_{i0} are the heatcapacity and the density of the substance of the solid phase. The components of the frictional force F_x and F_y are determined as follows [4]:

$$F_{xi} = \frac{3}{4}\frac{\alpha_i}{(2r_i)} C_d \rho \sqrt{(u-u_i)^2 + (v-v_i)^2}\,(v-v_i),$$

$$F_{yi} = \frac{3}{4}\frac{\alpha_i}{(2r_i)} C_d \rho \sqrt{(u-u_i)^2 + (v-v_i)^2}\,(v-v_i),$$

$$C_{di} = C_{di}^0 \psi(M_{i0})\varphi(\alpha_i), \quad C_{di}^0 = \frac{24}{\mathrm{Re}_{i0}} + \frac{4}{\mathrm{Re}_{i0}^{0.5}} + 0.4, \quad \psi(M_{i0}) = 1 + \exp\left(-\frac{0.427}{M_{i0}^{0.63}}\right),$$

$$\varphi(\alpha_i) = (1-\alpha_i)^{-2.5}, \quad \mathrm{Re}_{i0} = \rho \left|\overline{V} - \overline{V}_i\right| 2r_i / \mu, \quad M_{i0} = \left|\overline{V} - \overline{V}_i\right| / c,$$

$$\mathrm{Nu}_i = 2\exp(-M_{i0}) + 0.459\mathrm{Re}_{i0}^{0.55}\mathrm{Pr}^{0.33}, \quad \mathrm{Pr} = \gamma C_p \mu/\lambda, \quad 0 \le M_{i0} \le 2, \quad 0 \le \mathrm{Re}_{i0} < 2\cdot 10^5.$$

The temperature of the carried medium is found from the relation

$$T = (\gamma - 1)(e/\rho - 0.5(u^2 + v^2))/R.$$

The internal energy of the solid phase suspended in the gas is determined as

$$e_i = \rho_i C_{pi} T_i.$$

The energy equation for the carrier phase involves the thermal conductivity of the gas λ and the heat flux due to the heat exchange between the gas and the particle

$$Q_i = \alpha^T 4\pi r_i^2 (T - T_i) n = 6\alpha_i \mathrm{Nu}_i \lambda (T - T_i)/(2r_i)^2,$$

where $\mathrm{Nu}_i = 2r_i\alpha^T/\lambda$ is the Nusselt number, n is the concentration, and r_i is the radius of particles. Let the computational domain in variables (ξ, η, t) represent a unit square. The physical region (x, y, t) is mapped onto the unit square in which we introduce a uniform discretization along the ξ and η axes. The computational domain contains N_j nodes in the ξ direction and N_k nodes in the η direction. We denote unperturbed values of the density and of the velocity of sound in the gas and the characteristic linear dimension of the problem by ρ_0, c, and L. Dimensionless variables will be denoted by a ~ above them. Then we obtain $\rho = \rho_{i0}\tilde{\rho}_i$, $u = c\tilde{u}_i$, $v = c\tilde{v}_i$, $p = p_0 c^2 \tilde{p}$, $x = L\tilde{x}$, $y = L\tilde{y}$, $t = (L/c)\tilde{t}$, and $T = \tilde{T}/\rho_0 c^3 L$. We substitute these expressions into the equations of continuity, momentum, and energy of the gas. To reduce the equations of motion of the particles′ fraction to a dimensionless form we use the relations $\rho_i = \rho_{i0}\tilde{\rho}_i$, $u_i = c\tilde{u}_i$, $v_i = c\tilde{v}_i$, and $e_i = (\rho_{i0} C_{pi} T_{i0})\tilde{e}$, where ρ_{i0} is the unperturbed density of the fraction of particles, $\rho_i = \alpha_i \rho_{i0}$, α_i is the initial volume content of the solid fraction, ρ_{i0} is the density of the substance of the solid phase, and C_{pi} and T_{i0} are the specific heat and the solid-phase temperature selected for making the above equations dimensionless. Next, the system of the equations of motion of a two-phase multivelocity multitemperature polydisperse mixture is written in generalized moving coordinates [5–7]:

$$\mathbf{q}_t + \mathbf{E}_\xi + \mathbf{F}_\eta = \mathbf{H}, \tag{3}$$

$$\mathbf{E} = \frac{1}{J}\begin{bmatrix} \xi_t\rho + \xi_x\rho u + \xi_y\rho v \\ \xi_t\rho_1 + \xi_x\rho_1 u_1 + \xi_y\rho_1 v_1 \\ \cdots\cdots\cdots\cdots\cdots\cdots\cdots\cdots \\ \xi_t\rho_n + \xi_x\rho_n u_n + \xi_y\rho_n v_n \\ \xi_t\rho u + \xi_x\left(\rho u^2 + p - \tau_{xx}\right) + \xi_y\left(\rho uv - \tau_{xy}\right) \\ \xi_t\rho v + \xi_x\left(\rho uv - \tau_{xy}\right) + \xi_y\left(\rho v^2 + p - \tau_{yy}\right) \\ \xi_t\rho_1 u_1 + \xi_x\left(\rho_1 u_1^2\right) + \xi_y\left(\rho_1 u_1 v_1\right) \\ \cdots\cdots\cdots\cdots\cdots\cdots\cdots\cdots \\ \xi_t\rho_n u_n + \xi_x\left(\rho_n u_n^2\right) + \xi_y\left(\rho_n u_n v_n\right) \\ \xi_t\rho_1 v_1 + \xi_x\left(\rho_1 u_1 v_1\right) + \xi_y\left(\rho_1 v_1^2\right) \\ \cdots\cdots\cdots\cdots\cdots\cdots\cdots\cdots \\ \xi_t\rho_n v_n + \xi_x\left(\rho_n u_n v_n\right) + \xi_y\left(\rho_n v_n^2\right) \\ \xi_t e + \xi_x\left(\left(e + p - \tau_{xx}\right)u - \tau_{xy}v + \lambda\,\partial T/\partial x\right) \\ + \xi_y\left(\left(e + p - \tau_{yy}\right)v - \tau_{xy}u + \lambda\,\partial T/\partial y\right) \\ \xi_t e_1 + \xi_x\left(e_1 u_1\right) + \xi_y\left(e_1 v_1\right) \\ \cdots\cdots\cdots\cdots\cdots\cdots\cdots\cdots \\ \xi_t e_n + \xi_x\left(e_n u_n\right) + \xi_y\left(e_n v_n\right) \end{bmatrix}; \quad \mathbf{F} = \frac{1}{J}\begin{bmatrix} \eta_t\rho + \eta_x\rho u + \eta_y\rho v \\ \eta_t\rho_1 + \eta_x\rho_1 u_1 + \eta_y\rho_1 v_1 \\ \cdots\cdots\cdots\cdots\cdots\cdots\cdots\cdots \\ \eta_t\rho_n + \eta_x\rho_n u_n + \eta_y\rho_n v_n \\ \eta_t\rho u + \eta_x\left(\rho u^2 + p - \tau_{xx}\right) + \eta_y\left(\rho uv - \tau_{xy}\right) \\ \eta_t\rho v + \eta_x\left(\rho uv - \tau_{xy}\right) + \eta_y\left(\rho v^2 + p - \tau_{yy}\right) \\ \eta_t\rho_1 u_1 + \eta_x\left(\rho_1 u_1^2\right) + \eta_y\left(\rho_1 u_1 v_1\right) \\ \cdots\cdots\cdots\cdots\cdots\cdots\cdots\cdots \\ \eta_t\rho_n u_n + \eta_x\left(\rho_n u_n^2\right) + \eta_y\left(\rho_n u_n v_n\right) \\ \eta_t\rho_1 v_1 + \eta_x\left(\rho_1 u_1 v_1\right) + \eta_y\left(\rho_1 v_1^2\right) \\ \cdots\cdots\cdots\cdots\cdots\cdots\cdots\cdots \\ \eta_t\rho_n v_n + \eta_x\left(\rho_n u_n v_n\right) + \eta_y\left(\rho_n v_n^2\right) \\ \eta_t e + \eta_x\left(\left(e + p - \tau_{xx}\right)u - \tau_{xy}v + \lambda\,\partial T/\partial x\right) \\ + \eta_y\left(\left(e + p - \tau_{yy}\right)v - \tau_{xy}u + \lambda\,\partial T/\partial y\right) \\ \eta_t e_1 + \eta_x\left(e_1 u_1\right) + \eta_y\left(e_1 v_1\right) \\ \cdots\cdots\cdots\cdots\cdots\cdots\cdots\cdots \\ \eta_t e_n + \eta_x\left(e_n u_n\right) + \eta_y\left(e_n v_n\right) \end{bmatrix};$$

$$\mathbf{q} = \left[\frac{\rho}{J}, \frac{\rho_1}{J}, \ldots, \frac{\rho_n}{J}, \frac{\rho u}{J}, \frac{\rho v}{J}, \frac{\rho_1 u_1}{J}, \ldots, \frac{\rho_n u_n}{J}, \frac{\rho_1 v_1}{J}, \ldots, \frac{\rho_n v_n}{J}, \frac{e}{J}, \frac{e_1}{J}, \ldots, \frac{e_n}{J}\right]^T;$$

$$J = \begin{vmatrix} \xi_x & \xi_y & \xi_t \\ \eta_x & \eta_y & \eta_t \\ 0 & 0 & 1 \end{vmatrix}, \qquad \begin{aligned} \xi_t &= -x_t\xi_x - y_t\xi_y, \\ \eta_t &= -x_t\eta_x - y_t\eta_y; \end{aligned}$$

$$\mathbf{H} = \frac{1}{J}\begin{bmatrix} 0 \\ 0 \\ \cdots\cdots\cdots\cdots\cdots\cdots\cdots\cdots \\ 0 \\ -\sum\limits_{i=1,n} \breve{F}_{xi} + \alpha\partial p/\partial x \\ -\sum\limits_{i=1,n} \breve{F}_{yi} + \alpha\partial p/\partial x \\ \breve{F}_{x1}\rho_0/\rho_{10} - \alpha(\partial p/\partial x)\rho_0/\rho_{10} \\ \cdots\cdots\cdots\cdots\cdots\cdots\cdots\cdots \\ \breve{F}_{xn}\rho_0/\rho_{n0} - \alpha(\partial p/\partial x)\rho_0/\rho_{n0} \\ \breve{F}_{y1}\rho_0/\rho_{10} - \alpha(\partial p/\partial y)\rho_0/\rho_{10} \\ \cdots\cdots\cdots\cdots\cdots\cdots\cdots\cdots \\ \breve{F}_{yn}\rho_0/\rho_{n0} - \alpha(\partial p/\partial y)\rho_0/\rho_{n0} \\ -\sum\limits_{i=1,n} \hat{Q}_i - \sum\limits_{i=1,n}\left(\left|\breve{F}_{xi}\right|(u - u_i) - \left|\breve{F}_{yi}\right|(v - v_i)\right) + \alpha\partial(pu)/\partial x + \alpha\partial(pv)/\partial y \\ \hat{Q}_1 \\ \cdots\cdots\cdots\cdots \\ \hat{Q}_n \end{bmatrix}.$$

Here and in what follows we do not use a ~ to denote variables in dimensionless form. The pressure of the carrier medium has been determined above. The components of the frictional force $\breve{F}_x$ and $\breve{F}_y$, and also the heat fluxes on the right-hand sides of the energy equation for the fraction of the gas and the fraction of particles are determined as follows:

$$\breve{F}_{xi} = \frac{3}{4}\frac{\alpha_i}{(2r_i)} C_d \rho \sqrt{(u-u_i)^2 + (v-v_i)^2}\ (u-u_i) L \big/ \rho_0 c^2 ,$$

$$\breve{F}_{yi} = \frac{3}{4}\frac{\alpha_i}{(2r_i)} C_d \rho \sqrt{(u-u_i)^2 + (v-v_i)^2}\ (v-v_i) L \big/ \rho_0 c^2 ,$$

$$\hat{Q}_i = Q_i L \big/ \rho_0 c^3 , \quad \hat{Q}_i = Q_i \left(L \big/ \rho_0 c^3\right)\left(\rho_0 c^3 \big/ L\right) L \big/ \rho_{i0} C_{Ti} T_{i0} c = \hat{Q}_i \frac{\rho_0}{\rho_{i0}} \frac{c^2}{C_{Ti} T_{i0}} .$$

Here the physical region of flow in variables (x, y, t) is mapped onto the canonical computational domain in variables (ξ, η, t) [6, 7]. On the right-hand side of the system, we have introduced the notation of space derivatives: $\partial/\partial x = \xi_x \partial/\partial\xi + \eta_x \partial/\partial\eta$ and $\partial/\partial y = \xi_y \partial/\partial\xi + \eta_y \partial/\partial\eta$. System (1) in the domain with variable boundaries has been solved by the McCormack explicit method of second order in generalized moving coordinates [5–7] with a nonlinear-correction scheme [8].

Model of Coagulation of Aerosol Particles. Under the assumption of collinearity of the velocities of particles as they approach each other and coalesce in all cases of contact, the equations for the evolution of the characteristics of dispersity of the gas suspension, such as mass, concentration, momentum, and temperature, may be written as follows [2].

The mass m_i of the ith (i = 2, …, n) particle grows due to the absorption of smaller jth particles with a mass m_j (j = 1, 2, …, i – 1): $\dfrac{dm_i}{d\tau} = \sum\limits_{j=1}^{i-1} k_{ij} n_j m_j$, where $k_{ij} = (d_i + d_j)^2 |w_j - w_i|$ is the coagulation constant. The new value of the mass of particles of the ith fraction at the running node of the finite-difference grid makes it possible to determine a new value of the particle radius r_i. The decrease in the concentration of the ith particles due to their absorption by larger jth particles ($j = i + 1, i + 2, \ldots, n$) is described by the equation $\dfrac{du_i}{d\tau} = -n_i \sum\limits_{j=i+1}^{n} k_{ij} n_j$, ($i$ = 1, 2, …, n – 1). The new value of the volume content of the ith fraction changed due to coagulation is determined as $\alpha_i = 4 \big/ 3\pi r_i^3 n_i$. The concentration n_i is determined by the average density and the radius of the ith fraction on each step of computations. The coalescence of small particles with larger ones causes their velocity to change: $\dfrac{dw_i}{d\tau} = \dfrac{1}{m_i} \sum\limits_{j=1}^{i-1} k_{ij} (w_j - w_i) m_j n_j$. The temperature of a particle of the ith fraction, after the coagulation with particles of finer fractions, is found from the relation $T = \dfrac{1}{Cm}\left(\sum\limits_{j=1}^{i-1} k_{ij} n_j C_j m_j T_j + C_i m_i T_i\right)$, where T, C, and m are the temperature, the specific mass heat, and the mass of the particle of the ith fraction after the coagulation, and T_i, C_i, and m_i are the same parameters before coagulation. Coagulation-induced changes in the velocity and temperature of the dispersed phase are taken account of on each time step of the basic algorithm.

Results of Calculations of Vibrations of the Gas Suspension in an Acoustic Resonator. An acoustic resonator represents a closed plane channel of length L (Fig. 1). At the point x = 0, there is a piston that moves according to the harmonic law $x(t) = A(1 - \cos(2\pi f t))$, where A and f are the amplitude and frequency of piston vibrations. In the calculations given below, we have L = 1 m, d = 0.06 m, and A = 0.02 m. Let, at the initial instant of time, the gas suspension consisting of five fractions with particle radii r_{10} = 1 μm, r_{20} = 5 μm, r_{30} = 10 μm, r_{40} = 15 μm, and r_{50} = 20 μm be quiescent and, in a suspended state, fill uniformly the plane channel (Fig. 1). The density of the particles′ is $\rho_{10} = \rho_{20} = \rho_{30} = \rho_{40} = \rho_{50}$ = 1000 kg/m^3. The initial average density of dispersed fractions is $\rho_1 = \rho_2 = \rho_3 = \rho_4 = \rho_5$ = 0.000025 kg/m^3; the air density is ρ_0 = 1.21 kg/m^3. The temperature of the carrier and dispersed phases at the initial instant of time is T = 343 K. The specific heat of the substance of the dispersed phase is C_p = 4.2 kJ/(kg·K). Adhesion conditions are set on the boundaries of the dispersed phase, including the piston surface, for the velocity of the carrier and dispersed fractions. Homogeneous boundary conditions of the second kind are set for all the remaining gasdynamic functions. At $t > 0$, the process of piston vibrations begins, which sets the carrier and dispersed phases in motion.

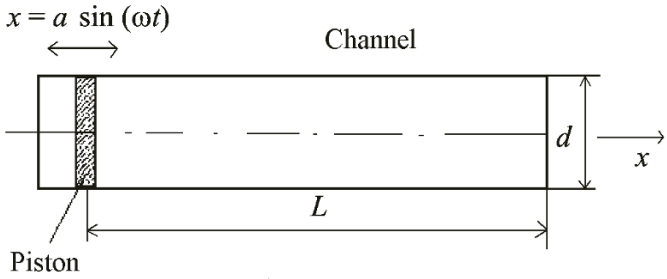

Fig. 1. Diagram of the resonator.

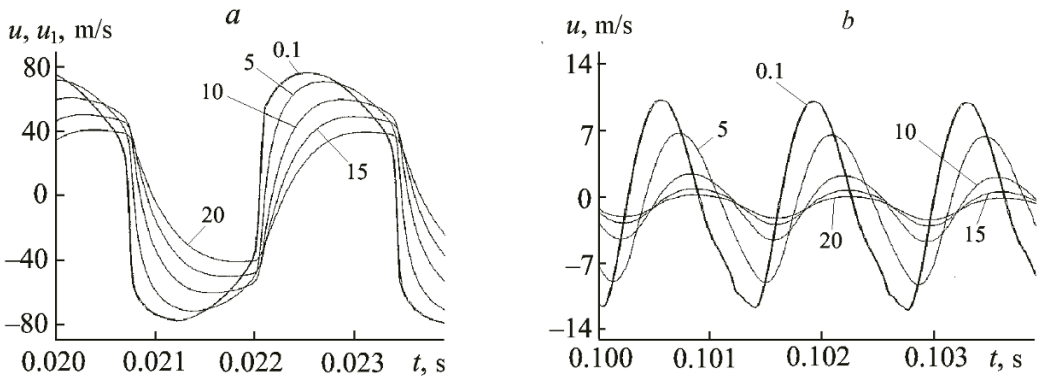

Fig. 2. Longitudinal velocity component vs. time at the point ($x = L/2$, $y = 0$): a) first eigenfrequency f_{11} and b) second eigenfrequency f_{12}.

Dynamics of the Gas Suspension in Exciting Vibrations at the First and Second Eigenfrequencies of Longitudinal Vibrations of a Gas Column. Figure 2 plots the longitudinal components of the velocity of the carrier phase and the dispersed phase (five fractions) versus time for two first eigenfrequencies of longitudinal vibrations of a gas column. The high-velocity slip of the carrier phase and of the finest fraction ($r_1 = 1$ μm) is minor; the velocity curves are very close (line 0.1). The amplitude of oscillations of the solid-phase velocity decreases with increase in the particle radius and the time lag of the change in the velocity of the dispersed phase behind that of the carrier medium increases.

Figure 3a–h gives the functions describing changes in the dispersity of the gas suspension due to coagulation. At the first eigenfrequency of vibrations of the gas column $f_{11} = c/2L$, at the center of the channel ($x = L/2$ and $y = d/2$), there is the antinode of the standing wave of the velocity field (Fig. 3a), whereas at the second eigenfrequency $f_{22} = c/L$, there are nodes on the ends and the center of the tube and antinodes at the points ($x = L/4$, $y = d/2$) and ($x = 3L/4$, $y = d/2$) where the amplitude of velocity oscillations acquire the largest values (Fig. 3b). Figure 3c shows the concentration distributions of aerosol particles of five fractions: from $r_0 = 1$ to 20 μm at the instant of time $t = 0.0575$ s. Next, the figure gives the initial radii and concentrations of dispersed fractions: $r_0 = 1$ μm and $\log N = 12.77$, 5 μm and $\log N = 10.67$, 10 μm and $\log N = 9.77$, 15 μm and $\log N = 9.24$, and 20 μm and $\log N = 8.87$.

By the instant of time $t = 0.0575$ s, the concentration of particles with $r_0 = 1$ μm along the channel, except for the end zones, decreases by approximately three orders of magnitude compared to the initial concentration. At the channel′s closed end where there is the node of the standing wave of the velocity field, the concentration of small particles decreases to a lesser extent, whereas at the piston the concentration of small particles decreases approximately 30 times compared to the initial one. With time, the concentrations of fractions with particle radii $r_0 = 1$, 10, and 15 μm become lower than the concentration of the coarsest fraction (Fig. 3c). In the vicinity of the antinode of the standing velocity wave, coagulation leads to a rapid growth in the size of the particles of all the fractions, except for the finest fraction, since the velocity nonequilibrium of dispersed phases in this region is the highest (Fig. 3e). Particle radii remain constant near the nodes ($x = 0$, $x = L$). At a constant concentration of the particles of the coarsest fraction ($r_0 = 20$ μm), the growth in the radius leads to a considerable increase in its average density. At the same time, the average density of fine fractions decreases throughout the resonator,

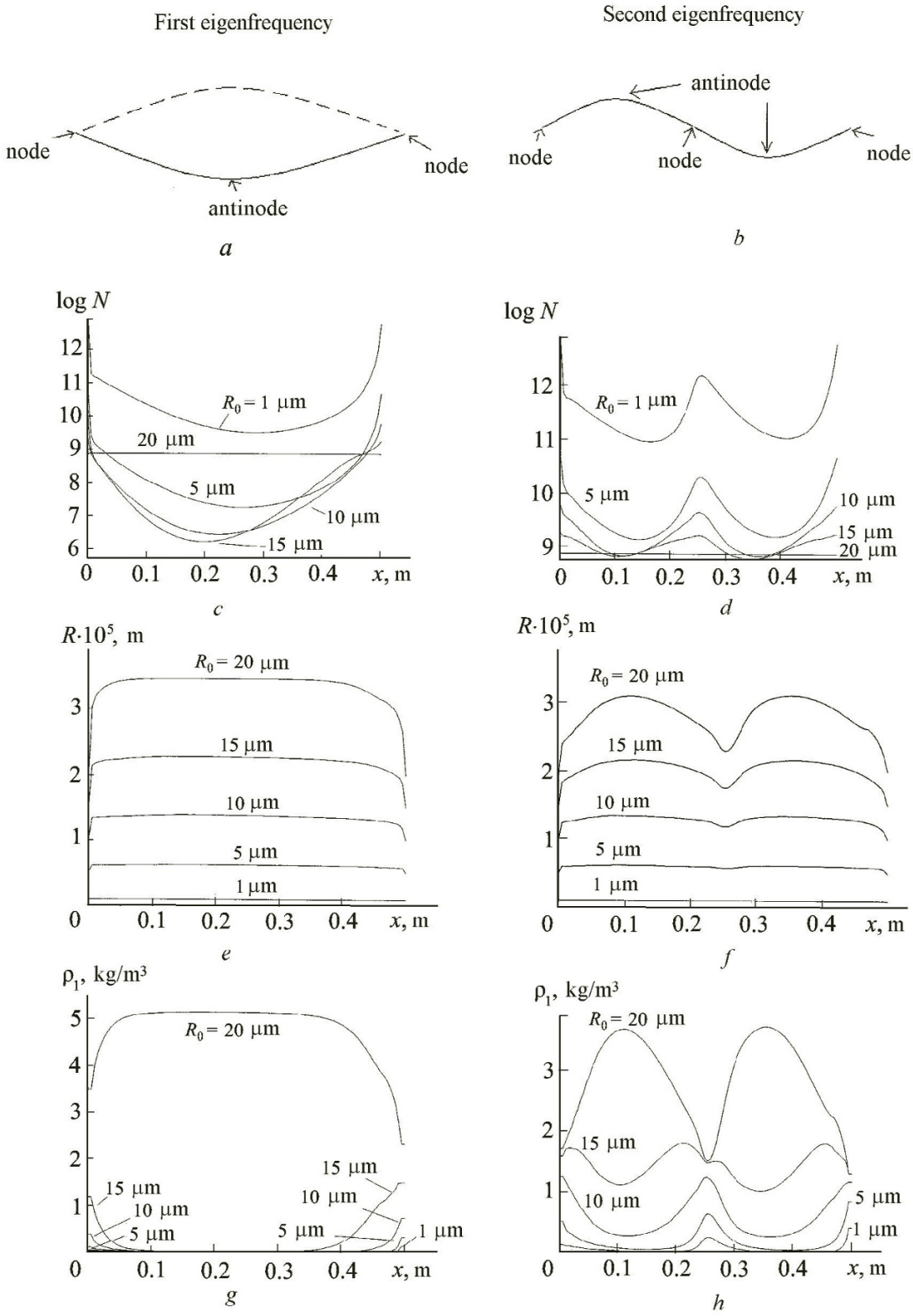

Fig. 3. Distributions of the nodes and antinodes of the standing wave of the gas-velocity field at the first (a) and second (b) eigenfrequencies of longitudinal vibrations of the gas column and concentrations (c and d), radii (g and h), and average densities (e and f) of aerosol particles of different fractions. Left, eigenfrequency f_{11}, right, eigenfrequency f_{21}.

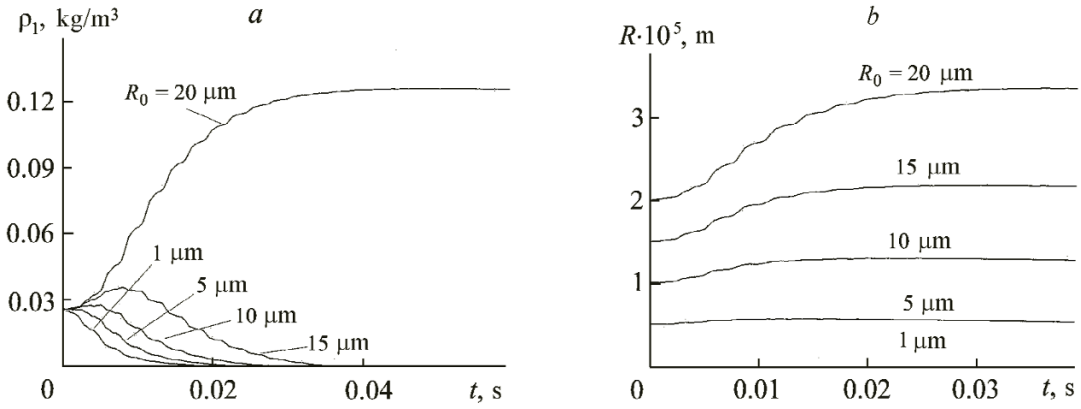

Fig. 4. Change in the average density of dispersed fractions (a) and in the radius of aerosol particles (b) at the point with coordinates ($x = L/2$, $y = d/2$) in vibrations at the first eigenfrequency.

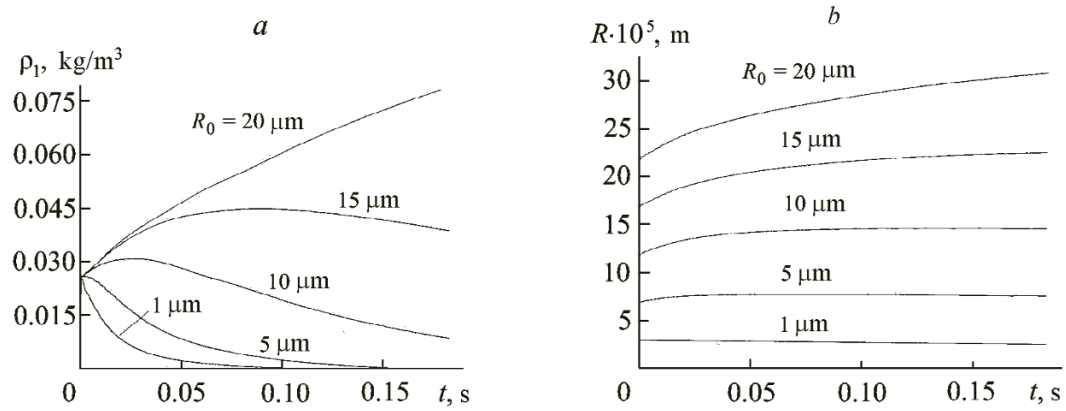

Fig. 5. Change in the average density of dispersed fractions (a) and in the radius of aerosol particles (b) at the point with coordinates ($x = L/2$, $y = d/2$) in vibrations at the second eigenfrequency.

except for the end zones, with time (Fig. 3g). Figure 4a and b plots the average densities of dispersed fractions and the radii forming these fractions at the point ($x = L/2$, $y = d/2$) versus time forpiston vibrations with a frequency f_{11}. The calculations show that the average density of the coarsest fraction (r_0 = 20 μm) grows monotonically with time, whereas the average density of the finest fraction (r_0 = 1 μm) decreases monotonically from the instant of time $t = 0$. For the remaining fractions, the initial stage of growth in the average density gives way to its decrease at a certain instant of time, which is attributed to the decrease in the concentration of the particles of these fractions due to the coagulation with larger particles. Here, the larger the particles of the fraction, the more lengthy the growth in its average density (Fig. 4a). By the instant of time t = 0.04 s, it is only the particles of the coarsest fraction that remain near the antinode of the standing wave of the velocity field ($x = L/2$) (Fig. 4a). The calculations show that the radii of the particles of all the fractions, except for the finest one, grow, taking the largest values by the instant of time $t = 0.04$ s. The particles of the coarsest fraction have the largest rate of growth (Fig. 4b).

Calculations of the dynamics of a polydisperse gas suspension at the instant of time $t = 0.03$ s in exciting vibrations at the second eigenfrequency are given in Fig. 3 on the right. At the midpoint of the channel, there is the node of the standing wave of the velocity field with the smallest amplitudes of velocities of the carrier fraction and dispersed fractions (Fig. 3b). For this reason, the process of coagulation in the vicinity of the node is slow and there is the local concentration maximum of

particles of all the fractions near it, except for the coarsest fraction (Fig. 3d). In the vicinity of the antinodes of the standing wave of the velocity field ($x = L/4$, $x = 3L/4$), the concentration of all the fractions, except for the coarsest one, is close to local minima (Fig. 3d) due to intense coagulation. To the concentration minima of the particles, there corresponds the maxima of the radii of particles of the coarser fractions, whereas in the region with the highest concentration there is the local minimum of the radii of aerosol particles of every size except for the finest fraction (Fig. 3f). The decrease in the concentration of all the fractions, except for the coarsest fraction, and growth in the radii of particles of all the fractions except for the finest one, result in the change in the average densities of the fractions (Fig. 3h). Here, the average density of the coarsest fraction is minimum at the nodes of the standing velocity-field wave, whereas for the remaining fractions, near the velocity nodes, there are the regions where the increased average density is preserved (Fig. 3h). Figure 5a and b plots the average density and the radius of particles of dispersed fractions versus time for piston vibrations at the second eigenfrequency f_{21}. We observe a growth in the average density of the coarse fraction ($r_0 = 20$ μm), which is monotonic with time, a monotonic decrease in the average density of the fine fraction ($r_0 = 1$ μm), and a nonmonotonic evolution of the average fraction of intermediate size (Fig. 5a). Coagulation leads to an increase in the effective radius of aerosol particles of all the fractions with time, except for the finest fractions (Fig. 5b).

Conclusions. Thus, coagulation of gas suspensions in the case of resonance vibrations in nonlinear wave fields makes it possible to efficiently decrease the concentration of fine fractions. This can be used as the preliminary stage before phase separation in inertial-type separators.

This work was carried out under Agreement No. 14.577.21.0151 of 28.11.2014 on the provision of a subsidy.

NOTATION

C_{pi} and ρ_{i0}, heat capacity and density of the substance of the ith fraction of the dispersed phase; e, total energy of the carrier phase; e_i, internal energy of the ith fraction of the dispersed phase; F_x and F_y, components of the interphase-friction force; n_i, concentration of particles of the ith fraction of the dispersed phase; Q, heat flux on the boundary between the aerosol particle and the gas; r_i, radius of aerosol particles of the ith fraction; u_i and v_i, Cartesian components of the velocity of the ith fraction of the dispersed phase; u and v, Cartesian components of the velocity of the carrier phase; T and T_i, temperatures of the carrier phase and of the ith fraction of the dispersed phase; α and α_i, volume content of the dispersed phase and of its ith fraction; λ and μ, thermal-conductivity and viscosity coefficients of the carrier phase; ρ, density of the gas; ρ_i, average density of the ith fraction of the dispersed phase.

REFERENCES

1. V. G. Tonkonog and S. N. Arslanova, *System for Feeding Cryogenic Fuel to a Power Plant*, RF Patent No. 2347934 (2009).
2. V. E. Alemasov, A. F. Dregalin, and V. A. Khudyakov, *Thermodynamic and Thermophysical Properties of Combustion Products: a Handbook in Five Volumes.* Vol. 1. *Calculation Methods* [in Russian], Proizvodstv.-Izd. Kombinat VINITI, Moscow (1971).
3. N. A. Gumerov and A. I. Ivandaev, Propagation of sound in polydisperse gas suspensions, *Prikl. Mekh. Tekh. Fiz*., No. 5, 115–124 (1988).
4. A. G. Kutushev, *Mathematical Modeling of Wave Processes in Aerodisperse and Powdery Media* [in Russian], Nedra, St. Petersburg (2003).
5. A. L. Tukmakov, Numerical modeling of vibrations of a monodisperse gas suspension in a nonlinear wave field, *Prikl. Mekh. Tekh. Fiz*., **52**, No. 2, 36–43 (2011).
6. C. Fletcher, *Computational Techniques for Fluid Dynamics*, Vol. 2 [Russian translation], Mir, Moscow (1991).
7. J. L. Steger, Implicit finite-difference simulation of flow about arbitrary two-dimensional geometries, *AIAA J.*, **16**, No. 7, 679−686 (1978).
8. A. I. Zhmakin and A. A. Fursenko, On a monotonic difference scheme of through counting, *Zh. Vych. Mat. Mat. Fiz*., **20**, No. 4, 1021–1031 (1980).